Smooth Connection of Trimmed NURBS Surfaces *

Pifu Zhang, Fuhua (Frank) Cheng
Graphics & Geometric Modeling Lab, Department of Computer Science
University of Kentucky, Lexington, Kentucky 40506-0046

Abstract. An automatic smooth surface connection method that has the capability of tension control is presented. Given two trimmed NURBS surfaces, the new method constructs a smooth *connection surface* to connect the trimming regions of the trimmed surfaces at the trimming curves. The connection satisfies the pseudo-G^1 or pseudo-C^1 smoothness requirement, a condition not as strong as G^1 or C^1, but smooth enough for most industrial applications. The construction process consists of four major steps: *connection curves construction and alignment*, *initial blends construction*, *setting up continuity constraints*, and *internal and external boundary smoothing*. The advantages of the new method include: (1) providing the users with more flexibility in adjusting the shape of the connection surface, (2) the representation of the connection surface is compatible with most of the current data-exchange standards, (3) including the classical blending as a special case but with more flexibility on the setting of the rail curves, and (4) smoother shape of the resulting connection surface through an energy optimization process. Test cases that cover important applications are included.

Keywords: constrained deformation, surface connection, blending, trimmed NURBS surfaces, rail curves, strain energy

1 Introduction

Surface connection refers to the process of smoothly connecting two or more surfaces, called *base surfaces*, with or without an auxiliary surface. The connection process is called *indirect connection* if an auxiliary surface, called a *connection surface*, is needed. Otherwise, it is called *direct connection*. In indirect connection, a connection surface is used to smoothly connect two or more disjoint base surfaces along *rail curves* specified by the user. In direct connection, the base surfaces are joined directly along a common boundary, called a *connection curve*. The smoothness of the connection process is usually established by requiring tangential continuity

*Research work of this project is supported by NSF (9912069).

between the base surfaces (for direct connection) or between the connection surface and the base surfaces (for indirect connection).

Direct connection is a frequently used process in industry. For instance, components of a complex shape (such as a car) may be designed by different groups separately or taken from deformed versions of some previously designed parts and then assembled into a complete object for efficiency purpose. Undesired positional or tangential discontinuity along the component boundary is usually fixed manually. This problem can be regarded as a *constrained surface deformation* problem by noticing that the connection process is equivalent to deforming the base surfaces so that the boundary curves of the base surfaces would coincide with the connection curve and appropriate continuity condition is satisfied along the connection curve. Techniques in this area can be found in [3][4][21][22][**?**].

The indirect connection problem has been extensively studied for two special cases. In the first case, the connection process is performed on the boundary curves of the base surfaces, i.e., the rail curves are defined by the boundary curves of the base surfaces. A typical example is the indirect connection of two cylinders with different diameters along their boundary curves. The connection surface is usually generated as a blending surface [1][12][13][**?**][20]. In some occasions, however, the connection surface is constructed by solving some interpolation condition [2][6][14]. The S-patch [16][17] and Gregory Patch [5], which can smoothly connect multiple surface patches, are constructed using a similar approach as well.

In the second case, the base surfaces are two intersecting surfaces and a connection surface is generated to replace the intersecting curve and its vicinity as a smoothing (rounding) process. The connection surface is usually a part of a canal surface generated by a rolling ball which has G^1 contact to the base surfaces. An extensive survey of results in this case can be found in [19]. Connection surfaces that have higher degree of continuity along the rail curves can also be constructed [9][10][11].

Indirect connection of parametric surfaces with general rail curves has not been well studied yet. Filip's work [8] seems to be the only known result in this area. Given two arbitrary rail curves, a connection surface that allows tension control is constructed using the Hermite interpolation technique. Since a tangent function usually can not be explicitly defined for an arbitrary rail curve, the connection surface constructed this way is not C^1 continuous, as the author has claimed, but only piecewise C^1 continuous. The most serious drawback of this approach, however, is that the connection surface does not have a NURBS representation and the degree of the surface is high. For bicubic B-spline base surfaces, the degree of the resulting connection surface is eighteen, not suitable for stable numerical computation.

We will overcome the problems encountered by Filip's approach by presenting a new approach for indirect connection of trimmed NURBS surfaces. The connection satisfies the pseudo-G^1 or pseudo-C^1 smoothness requirement (to be defined in Section 2), a condition not as strong as G^1 or C^1, but smooth enough for most industrial applications. Most importantly, the connection surface constructed by this method has a bicubic NURBS representation and, hence, is compatible with most of the current data-exchange standards. The connection surface is a composition of many small blends, instead of a single blend. Hence, it takes more space for internal representa-

tion. But the bicubic NURBS representation makes it more efficient and stable for computation and rendering, a seemingly reasonable trade-off. The new approach also allows tension control of the connection surface by the user.

The remaining part of the paper is arranged as follows. A formal description of the problem is given in Section 2. The basic idea of the proposed method is presented in Section 3. Techniques needed in constructing the connection surface are described in Sections 4-8. Test results of the proposed method, including a comparison of the new approach with Filip's approach, are included in Section 9. Concluding remarks are given in Section 10.

2 Problem Formulation

The problem considered in this paper can be described as follows: Given two trimmed surfaces $\mathbf{S}_0$ and $\mathbf{S}_1$ with trimming curves $\mathbf{T}_0$ and $\mathbf{T}_1$, respectively, construct a new surface $\mathbf{S}$ that connects the trimming regions of $\mathbf{S}_0$ and $\mathbf{S}_1$ at $\mathbf{T}_0$ and $\mathbf{T}_1$, respectively. $\mathbf{S}_0$ and $\mathbf{S}_1$ are called the *base surfaces* and $\mathbf{S}$ is called a *connection surface*. The trimming curves where the connection is performed are called the *connection curves*. The connection between the base surfaces and the connection surface should satisfy some smoothness condition along the connection curves. Due to the fact that popular smoothness conditions such as G^1 and C^1 continuity are not possible to achieve when $\mathbf{T}_0$ and $\mathbf{T}_1$ are arbitrarily defined, we will use a lower smoothness requirement for the connection process.

Definition. The connection between a connection surface and a base surface is said to be *pseudo-G^1* (*pseudo-C^1*) *continuous* if the connection is C^0 on the entire connection curve but G^1 (C^1) on finitely many points of the connection curve only. The points where the connection satisfies G^1 (C^1) condition must be densely populated over the connection curve so that the connection curve is contained in the union of the ϵ-neighborhoods of such points for some small positive number ϵ.

An example is shown in Figure 1 where a connection surface (in dark blue) connects two base surfaces (in green and sky blue) at two circular connection curves. The connection is pseudo-G^1 smooth.

The connection curves have been called *rail curves* in the blending process. However, since our connection process is more general than the classical blending process (which focuses on smoothly joining parametric surfaces along their boundary curves or offset curves of the boundary curves, see Figures 6 and 7), and these curves are not generated in the same way as the blending process, we choose not to use the same term here to avoid confusion.

The base surfaces $\mathbf{S}_0$ and $\mathbf{S}_1$ are NURBS surfaces of degrees p_0 and p_1 in u direction and degrees q_0 and q_1 in v direction, respectively,

$$\mathbf{S}_k(u,v) = \frac{\sum_{i=0}^{m_k}\sum_{j=0}^{n_k} w_{i,j}^k \mathbf{Q}_{i,j}^k N_{i,p_k}^k(u) N_{j,q_k}^k(v)}{\sum_{i=0}^{m_k}\sum_{j=0}^{n_k} w_{i,j}^k N_{i,p_k}^k(u) N_{j,q_k}^k(v)}, \tag{1}$$

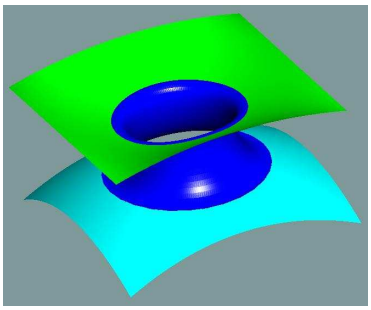

Figure 1: An example of smooth surface connection.

$$k = 0, 1 \qquad (u, v) \in [0, 1] \times [0, 1]$$

where $\mathbf{Q}^k_{i,j}$ are 3D control points, $N^k_{i,p_k}(u)$ and $N^k_{j,q_k}(v)$ are B-spline basis functions of degrees p_k and q_k, respectively, and $w^k_{i,j}$ are weight functions. $N_{i,p_k}(u)$ and $N_{j,q_k}(v)$ are defined with respect to the knot vectors $\tau^k = \{\tau^k_0, \tau^k_1, \ \ldots \ , \tau^k_{m_k+p_k+1}\}$, and $\sigma^k = \{\sigma^k_0, \sigma^k_1, \ \ldots \ , \sigma^k_{n_k+q_k+1}\}$, respectively, with $\tau^k_0 = ... = \tau^k_{p_k} = \sigma^k_0 = ... = \sigma^k_{q_k} = 0$ and $\tau^k_{m_k+1} = ... = \tau^k_{m_k+p_k+1} = \sigma^k_{n_k+1} = ... = \sigma^k_{n_k+q_k+1} = 1$.

A trimming curve of a free-form surface may be defined by a closed parametric curve in the domain of the surface. However, in industrial applications, a trimming curve is usually defined by a set of points in the domain of the surface, due to the fact that trimming curves are usually generated through the surface-surface intersection operation. We follow the industrial standard in this work, i.e., the trimming curves $\mathbf{T}_k$, $k = 0, 1$, are defined by closed linear polygons in the domains of $\mathbf{S}_k$ with l_k vertices $\mathbf{V}^k_0$, $\mathbf{V}^k_1$, $\mathbf{V}^k_2$, ... , $\mathbf{V}^k_{l_k} = \mathbf{V}^k_0$, $k = 0, 1$, respectively. The trimming curves do not intersect themselves. The trimming region of a trimmed NURBS surface is determined by the *curve handedness rule*, i.e., a point is in the trimming region if it is on the left side when one traverses the trimming curve.

The connection surface $\mathbf{S}$ should connect the trimming regions of the given trimmed NURBS surfaces at the trimming curves. The connection should be at least pseudo-G^1 or pseudo-C^1 continuous. The connection surface should have a NURBS representation to be compatible with the current data-exchange standards. The shape of the connection surface should be smooth enough to meet design criteria. Besides, the user should be able to control the shape of the connection surface through some simple mechanism to satisfy both aesthetic and areodynamic requirements.

3 Basic idea

The main idea of the new approach is to construct the connection surface as a set of (small) blends instead of a single blend. The small blends are constructed by splitting the trimming curves of

the base surfaces into small, aligned segments and then blending corresponding segments with an appropriate profile curve to form initial blends. The connection surface is formed by piecing the small blends together through an optimization process to achieve internal and external smoothness requirements. Since each small blend is a bicubic Bézier patch, the resulting connection surface is a composite Bézier surface and, consequently, a bicubic NURBS surface. The user can control the shape of the blends and the connection surface by manipulating a tension parameter contained in the profile curve.

The main steps of our approach are show below:

1. Connection curves construction and alignment;
2. Initial blending construction;
3. Setting up continuity control constraints;
4. Shape optimization.

The first step is the most critical step because the result of this step determines the shape of the blends constructed in the second step and, hence, essentially the shape of the connection surface. Details of the above steps are given in the subsequent sections.

4 Connection Curves Construction and Alignment

A trimming curve, represented as a (closed) linear polygon in the parameter space of the trimmed surface, can not be used as a connection curve directly. A connection curve has to be constructed separately. An intuitive approach is to construct a cubic B-spline or piecewise Bézier curve that interpolates the vertices of the trimming curve in the parameter space and use its image under the surface definition as the connection curve [8]. This conection curve, however, can not be used in the subsequent blend construction process because, after the mapping of the surface definition, it is no longer a B-spline or a piecewise Bézier curve. Besides, a connection curve constructed this way has a degree of 18, not suitable for stable numerical computation.

The connection curves will be constructed in the modeling space directly. These curves must satisfy the following requirements:

1. they have the same number of curve segments and their segments are properly aligned;
2. the number of curve segments is big enough so that each connection curve can be covered by the ϵ-neighborhoods of the endpints of its curve segments;
3. each connection curve lies exactly on the corresponding base surface.

The first requirement is to ensure components of the connection surface are properly constructed (Section 5) and satisfy the aesthetic and areodynamic requirements on their shape. The second requirement is to ensure pseudo-G^1 continuity between the connection surface and the base surfaces. The third requirement is to ensure that there is no gap between the connection surface and the base surfaces. The construction process is shown below.

First, for each base surface $\mathbf{S}_k$, $k = 0, 1$, we construct a cubic B-spline curve $\mathbf{C}_k$ that interpolates the vertices of the trimming curve $\mathbf{T}_k$ in the modeling space $\mathbf{S}_k(\mathbf{V}_i^k)$, $i = 0, 1, ..., l_k$, as follows:

$$\mathbf{C}_k(t) = \sum_{j=0}^{l_k+2} N_{j,3}^k(t)\mathbf{P}_j^k \qquad t \in [t_3, t_{l_k+3}] = [0, 1] \tag{2}$$

where $\mathbf{P}_j^k$ are 3D control points and $N_{j,3}^k(t)$ are cubic B-spline basis functions defined with respect to the knot vector $t^k = \{t_0^k, t_1^k, \ ... \ , t_{l_k+6}^k\}$. The knots are defined using the interpolation points $\mathbf{S}_k(\mathbf{V}_i^k)$, following the centripetal model [15]. The control points $\mathbf{P}_j^k$ are computed by solving the following system of equations:

$$\mathbf{C}_k(t_i) = \sum_{j=0}^{l_k+2} N_{j,3}^k(t_i)\mathbf{P}_j^k = \mathbf{S}_k(\mathbf{V}_{i-3}^k), \tag{3}$$

$$i = 3, 4, ..., l_k + 3.$$

$\mathbf{C}_k(t)$ is a closed curve, its control points are cyclic, i.e., $\mathbf{P}_j^k = \mathbf{P}_{j \ mod \ l_k}^k$.

To meet the first and the second requirements, let $\mathbf{P}_{ctd}^k$ and $\mathbf{N}_{ctd}^k$ be the *centroid* and *normal vector* of the trimming curve $\mathbf{T}_k$ defined as follows:

$$\mathbf{P}_{ctd}^k = \frac{1}{l_k}\sum_{i=1}^{l_k} \mathbf{S}_k(\mathbf{V}_i^k), \qquad k = 0, 1 \tag{4}$$

and

$$\mathbf{N}_{ctd}^k = \frac{1}{l_k}\sum_{i=1}^{l_k} \mathbf{N}_i^k, \qquad k = 0, 1 \tag{5}$$

where $\mathbf{N}_i^k$ are the normal vectors of the trimmed surface $\mathbf{S}_k$ at $\mathbf{S}_k(\mathbf{V}_i^k)$. Using these four items, one can construct a cubic Bézier curve $\mathbf{C}(t)$ ($t \in [0, 1]$) with $\mathbf{P}_{ctd}^0$ and $\mathbf{P}_{ctd}^1$ as its endpoints and $\mathbf{N}_{ctd}^0$ and $\mathbf{N}_{ctd}^1$ as its endpoint tangent vectors. This curve is the *centroid line* of the connection surface to be constructed. Using the first derivative and the second derivative of the curve $\mathbf{C}(t)$ at the endpoints, one can construct a plane through each endpoint. Each plane has two or more intersection points with the corresponding connection curve. Take the two outmost intersection points on each connection curve and recursively subdivide the left and the right portions of the connection curves concurrently to generate a set of points $\mathbf{D}_i^k$, $i = 0, 1, 2, ..., N$, on the connection curves with $\mathbf{D}_0^k = \mathbf{D}_N^k$, $k = 0, 1$. The subdivision process stops when the following two conditions are satisfied: (1) the Euclidean distance between each pair of consecutive points is less than $\epsilon/2$, and (2) for each resulting sub-segment of the connection curves, the distance between the chord and the arc is less than $\epsilon/2$. If a pair of consecutive points fail to satisfy any of these conditions,

the corresponding segments on both connection curves are further recursively subdivided until these conditions are satisfied by subsegments on both connection curves.

When the subdivision process stops, we construct a closed cubic B-spline curve to interpolate $\mathbf{D}_i^0$, $i = 0, 1, 2, ..., N$, and a closed cubic B-spline curve to interpolate $\mathbf{D}_i^1$, $i = 0, 1, 2, ..., N$. These curves are (slightly) different from $\mathbf{C}_0$ and $\mathbf{C}_1$. For simplicity, however, we shall use $\mathbf{C}_0$ and $\mathbf{C}_1$ to represent these curves again. The new $\mathbf{C}_0$ and $\mathbf{C}_1$ will be used as the connection curves for the base surfaces $\mathbf{S}_0(u, v)$ and $\mathbf{S}_1(u, v)$, respectively. Note that, with $\mathbf{D}_i^k$, $i = 0, 1, 2, ..., N$, as interpolation points, $\mathbf{C}_0$ and $\mathbf{C}_1$ satisfy requirements 1 and 2 now. In general, the curve $\mathbf{C}_k(t)$ does not lie on the base surface $\mathbf{S}_k$.

To meet the third requirement, we deform the base surface $\mathbf{S}_k(u, v)$ so that the deformed version would contain the connection curve $\mathbf{C}_k$. This process will be performed as a constrained optimization process to ensure (1) the difference between the deformed base surface and the original base surface is as small as possible, and (2) the shape and curvature distribution of the deformed base surface are as close to the original base surface as possible. Obviously, the objective function of the optimization process should be constructed based on the difference of the deformed version and the given version of the base surface.

For each base surface $\mathbf{S}_k$, $k = 0, 1$, let $\bar{\mathbf{S}}_k$ be the deformed version of the base surface. The displacement function is therefore

$$\mathbf{V}_k(u, v) = \mathbf{S}_k(u, v) - \bar{\mathbf{S}}_k(u, v). \tag{6}$$

To ensure that after the deformation process the connection curve $\mathbf{C}_k$ would lie on the deformed base surface $\bar{\mathbf{S}}_k$ completely, one can consider a positive definite error functional as follows:

$$\delta = 1/2 \int_0^1 (\mathbf{C}_k(t) - \bar{\mathbf{S}}_k(\hat{\mathbf{C}}_k(t))^2 dt$$

where $\hat{\mathbf{C}}_k(t)$ is a parametric curve in the domain of the base surface $\mathbf{S}_k$. The value of this error functional is zero and a minimum when the curve $\mathbf{C}_k(t)$ is equal to the curve $\bar{\mathbf{S}}_k(\hat{\mathbf{C}}_k(t))$, i.e., when the connection curve is the image of the deformed surface of some parametric curve in the domain of the surface. A natural choice for $\hat{\mathbf{C}}_k(t)$ is the cubic B-spline curve that interpolates the vertices of the trimming curve $\mathbf{T}_k$ in the domain of $\mathbf{S}_k$. Following a technique of Celniker and Welch [4], the above error functional can be transformed to a linear constraint as follows by requiring its value to be a minimum – that is, its gradient with respect to the control points to be 0.

$$BQ = \mathbf{b} \tag{7}$$

Q is the set of control points of the deformed surface $\bar{\mathbf{S}}_k$.

The deformed surface is computed by performing constrained optimization on the thin plate energy model of the displacement function. The optimization process will be discussed in Section 8. The deformed surface now satisfies all three requirements. Note that the difference between $\mathbf{C}_k(t)$ and $\bar{\mathbf{C}}_k(t)$ is small. Hence, the difference between the deformed version and the original version of the base surface is small too. For simplicity, after this point we shall use $\mathbf{S}_k(t)$, not $\bar{\mathbf{S}}_k$, to refer to its deformed version.

5 Initial Blends Construction

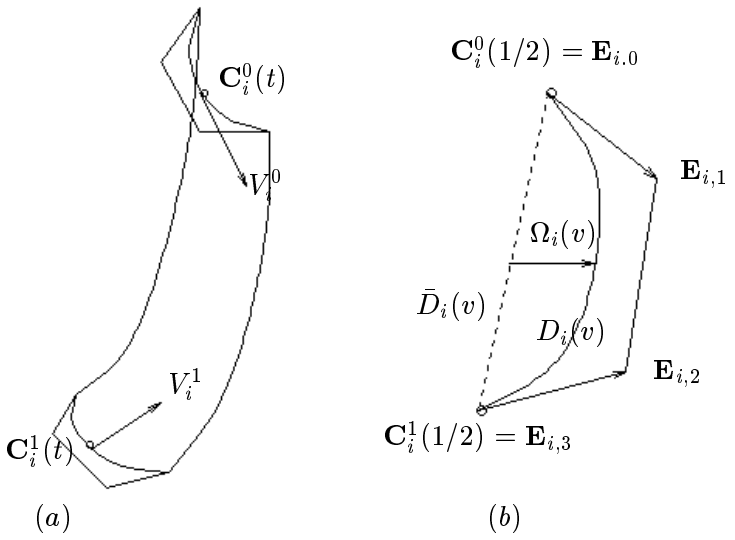

Figure 2: Construction of a profile curve.

Using the points $\mathbf{D}_i^k$ $(i = 1, 2, ...N-1)$, $k = 0, 1$, generated in the previous step, one can subdivide each of the connection curves $\mathbf{C}_k(t)$, $k = 0, 1$, into N cubic Bézier curve segments: $\mathbf{B}_0^k(t)$, $\mathbf{B}_1^k(t)$, ..., $\mathbf{B}_{N-1}^k(t)$ where $t \in [0, 1]$. The goal of this step is to construct a blend $\hat{\mathbf{S}}_i(u, v)$ for each pair of corresponding Bézier curve segments, $\mathbf{B}_i^0(t)$ and $\mathbf{B}_i^1(t)$ $(i = 0, ..., N-1)$, of the connection curves. Combined, these blends will form the initial shape of the connection surface.

An intuitive approach one can think of immediately is the Hermite Interpolation technique, that is, constructing the blend $\hat{\mathbf{S}}_i(u, v)$ as follows:

$$\begin{aligned}\hat{\mathbf{S}}_i(u,v) &= H_0(v)\mathbf{B}_i^0(u) + H_1(v)\mathbf{B}_i^1(u) \\ &+ H_2(v)\mathbf{D}_i^0(u) + H_3(v)\mathbf{D}_i^1(u)\end{aligned} \tag{8}$$

where $H_i(v)$ are cubic Hermite basis functions

$$\begin{aligned} H_0(v) &= v^2(2v-3)+1; \qquad H_1(v) = 1 - H_1(v); \\ H_2(v) &= v(v-1)^2; \qquad\quad H_3(v) = v^2(v-1) \end{aligned}$$

and $\mathbf{D}_i^0(u)$ and $\mathbf{D}_i^1(u)$ are tangent functions to be defined. This is essentially what was done by Filip [8]. The representation of the resulting connection surface in this case is not compatible with that of the base surfaces. Note that unless $\mathbf{D}_i^0(u)$ and $\mathbf{D}_i^1(u)$ are explicitly defined, the smoothness between the connection surface and the base surfaces is not G^1, as Filip has claimed in [8]. In the following, we present an approach that provides a compatible representation for the resulting connection surface. The new approach embeds the shape information of the base surfaces into that of the connection surface in a more natural way. The resulting connection surface satisfies the pseudo-G^1 or pseudo-C^1 smoothness requirement at the connection curves.

For each pair of corresponding Bézier curve segments $\mathbf{B}_i^0(t)$ and $\mathbf{B}_i^1(t)$ $(i = 0, ..., N-1)$, we first find a vector V_i^k that is tangent to the surface $\mathbf{S}_k(u, v)$ and normal to the Bézier curve segment $\mathbf{B}_i^k(t)$ at the point $\mathbf{B}_i^k(1/2)$, $k = 0, 1$. There are two such vectors. We take the one that is going away from the trimming region of $\mathbf{S}_k(u, v)$ (see Figure 2(a)). We then define two points, $\mathbf{E}_{i,1}$ and $\mathbf{E}_{i,2}$, as follows (see Figure 2(b)):

$$\mathbf{E}_{i,1} = \mathbf{B}_i^0(1/2) + w_1 V_i^0,$$

$$\mathbf{E}_{i,2} = \mathbf{B}_i^1(1/2) + w_2 V_i^1$$

where w_0 and w_1, called *tension parameters*, are real numbers between 0 and 1. The four points $\mathbf{E}_{i,0} = C_i^0(1/2)$, $\mathbf{E}_{i,1}$, $\mathbf{E}_{i,2}$, and $\mathbf{E}_{i,3} = C_i^1(1/2)$ define a cubic Bézier curve as follows:

$$\mathbf{D}_i(v) = B_{0,3}(v)\mathbf{E}_{i,0} + B_{1,3}(v)\mathbf{E}_{i,1} +$$

$$B_{2,3}(v)\mathbf{E}_{i,2} + B_{3,3}(v)\mathbf{E}_{i,3}$$

where $B_{i,3}(v)$ are Bernstein basis functions of degree three. By using $\mathbf{E}_{i,0}$, $\mathbf{E}_{i,3}$, and two points in between, one can get a cubic Bézier curve representation for the line segment $\mathbf{E}_{i,0}\mathbf{E}_{i,3}$, as follows:

$$\bar{\mathbf{D}}_i(v) = B_{0,3}(v)\mathbf{E}_{i,0} + B_{1,3}(v)\bar{\mathbf{E}}_{i,1} +$$

$$B_{2,3}(v)\bar{\mathbf{E}}_{i,2} + B_{3,3}(v)\mathbf{E}_{i,3}$$

where $\bar{\mathbf{E}}_{i,1} = (2C_i^0(1/2) + C_i^1(1/2))/3$ and $\bar{\mathbf{E}}_{i,2} = (C_i^0(1/2) + 2C_i^1(1/2))/3$. $\bar{\mathbf{D}}_i(v)$ is the base segment of $\mathbf{D}_i(v)$ (see Figure 2 (b)). We then compute the vector $\Omega_i(v)$ that is the difference of $\mathbf{D}_i(v)$ and $\bar{\mathbf{D}}_i(v)$.

$$\Omega_i(v) = D_i(v) - \bar{D}_i(v)$$

Using a technique similar to the so called *blending between two cross-sections using one profile* [7], one can define a blending surface $\hat{S}_i(u, v)$ for $\mathbf{B}_i^0$ and $\mathbf{B}_i^1$, $i = 0, 1, ..., N-1$, as follows:

$$\hat{S}_i(u, v) = (1 - \phi(v))\mathbf{C}_i^0(u) + \phi(v)\mathbf{C}_i^1(u) + \Omega_i(v) \tag{9}$$

where $\phi(v)$ is a blending function defined as follows:

$$\phi(v) = B_{0,3}(v)\alpha_0 + B_{1,3}(v)\alpha_1 + B_{2,3}(v)\alpha_2 + B_{3,3}(v)\alpha_3$$

with $\alpha_0 = 0$, $\alpha_3 = 1$, and α_1 and α_2 are determined based on the shape of the base surfaces. If the angle between the vector V_i^0 and the base plane of the trimming curve $\mathbf{C}_0(t)$ (the plane that passes through the centroid of $\mathbf{C}_0(t)$ and is perpendicular to the normal of $\mathbf{C}_0(t)$) is θ_0, and the angle between the vector V_i^1 and the base plane of the trimming curve $\mathbf{C}_1(t)$ is θ_1, then α_1 and α_2 can be defined as follows (see Figure 3):

$$\alpha_1 = |V_i^0|\ w_1\ Sin(\theta_0) \tag{10}$$

$$\alpha_2 = \alpha_3 - |V_i^1|\ w_2\ Sin(\theta_1) \tag{11}$$

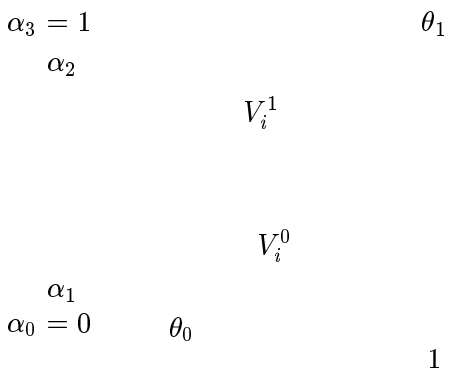

Figure 3: Construction of α_1 and α_2.

The blending surface $\hat{S}_i(u,v)$ defined in eq. (9) is a bicubic Bézier surface. If the control points of the Bézier curve segment $\mathbf{B}_i^k(u)$ are $P_0^{i,k}$, $P_1^{i,k}$, $P_2^{i,k}$ and $P_3^{i,k}$, $k = 0, 1$ and $i = 0, 1, ..., N-1$, then the control points of $\hat{S}_i(u,v)$, $\hat{\mathbf{Q}}_{j,l}^i$ $(j = 0, .., 3, l = 0, ..., 3)$, can be expressed as follows:

$$[\hat{\mathbf{Q}}_{j,l}^i] = \begin{bmatrix} P_0^{i,0} & P_0^{i,1} & 1 \\ P_1^{i,0} & P_1^{i,1} & 1 \\ P_2^{i,0} & P_2^{i,1} & 1 \\ P_3^{i,0} & P_3^{i,1} & 1 \end{bmatrix}$$

$$\begin{bmatrix} 1-\alpha_0 & 1-\alpha_1 & 1-\alpha_2 & 1-\alpha_3 \\ \alpha_0 & \alpha_1 & \alpha_2 & \alpha_3 \\ 0 & \mathbf{E}_{i,1} - \bar{\mathbf{E}}_{i,1} & \mathbf{E}_{i,2} - \bar{\mathbf{E}}_{i,2} & 0 \end{bmatrix}$$

A connection surface constructed this way would only satisfy C^0 continuity on it boundaries with the base surfaces and on the boundaries of the component surfaces. Smoother continuity condition will be achieved through an optimization process. This will be discussed in Section 8.

To get a good connection surface shape, the user needs to select proper values for the tension parameters, w_1 and w_2. In general, larger tension parameters will result in smoother connection surface shape. However, larger tension parameters sometimes could generate abnormal shapes such as cusps or loops on isoparametric curves of the connection surface. So these parameters sometimes have to be iteratively adjusted to find the best values. A suggesed initial value for these parameter is 0.5. A rule of thumb in adjusting these parameters is to decrease the values of the tension parameters if abnormal portions are found in the connection surface. Otherwise, increase the values of the tension parameters to get smoother connection surface. The maximum value for the tension parameters is one. At that point the connection surface is pseudo-C^1 continious.

6 Setting Up Continuity Constraints

The purpose of this step is to set up continuity constraints for the optimization process. Two types of continuity constraints will be considered: *interior continuity constraint* and *exterior continuity constraint*. The first one refers to continuity constraint between component surfaces of the connection surface, the second one refers to continuity constraint between the connection surface and the base surfaces.

6.1 Interior continuity constraint

Adjacent component surfaces of the connection surface are required to satisfy C^1 continuity on their boundaries. If two adjacent component surfaces $\hat{\mathbf{S}}_i(u,v)$ and $\hat{\mathbf{S}}_{i+1}(u,v)$, $0 <= i <= N-1$, have the same number of control points in v direction, then their control points must satisfy the following conditions:

$$\hat{\mathbf{Q}}^i_{n_i,l} = \hat{\mathbf{Q}}^{i+1}_{0,l}, \qquad l = 0,1,...,m_i \tag{12}$$

and

$$\hat{\mathbf{Q}}^i_{n_i,l} - \hat{\mathbf{Q}}^i_{n_i-1,l} = \hat{\mathbf{Q}}^{i+1}_{1,l} - \hat{\mathbf{Q}}^{i+1}_{0,l}., \qquad l = 0,1,...,m_i \tag{13}$$

In the above conditions, $i+1$ is modulo N.

Sometimes, due to surface shape requirement, adjacent component surfaces might have different number of control points in v direction, i.e., $m_i \neq m_{i+1}$. In that case, adjacent component surfaces must satisfy pseudo C^1 continuity on their boundaries, i.e.,

$$\hat{\mathbf{S}}_i(1,v^i_l) = \hat{\mathbf{S}}_{i+1}(0,v^i_l), \qquad l = 0,1,...,M \tag{14}$$

$$\frac{d}{du}\hat{\mathbf{S}}_i(1,v^i_l) = \frac{d}{du}\hat{\mathbf{S}}_{i+1}(0,v^i_l), \qquad l = 0,1,...,M \tag{15}$$

for some v^i_l, where $M \geq max(m_i, m_{i+1})$ and $|v^i_l - v^i_{l+1}| < \epsilon$. In the above conditions, $i+1$ is modulo N too.

6.2 Exterior continuity constraint

Constraint for continuity condition between the connection surface and the base surface is needed for v direction only. This will be set up in three steps.

First, for each component surface $\hat{\mathbf{S}}_k(u,v)$, $k = 0,1,...,N-1$, map the control points of its boundary curves $\hat{\mathbf{S}}_k(u,0)$ and $\hat{\mathbf{S}}_k(u,1)$ onto the boundary curves using the shortest distance technique. For instance, for the boundary curve $\hat{\mathbf{S}}_k(u,0)$, this is equivalent to the process of identifying the point $(u_{i,0},0)$ in the parameter space of $\hat{\mathbf{S}}_k(u,0)$ so that the distance between $\hat{\mathbf{Q}}^k_{i,0}$ and $\hat{\mathbf{S}}_k(u_{i,0},0)$ is the minimum, $i = 0,1,...,m_k$. $\hat{\mathbf{S}}_k(u_{i,0},0)$ is called the *image* of $\hat{\mathbf{Q}}^k_{i,0}$ on the curve $\hat{\mathbf{S}}_k(u,0)$. Note that $\hat{\mathbf{S}}_k(u_{i,0},0)$ is also a point on the connection curve $\mathbf{T}_0$ of the base surface $\mathbf{S}_0(u,v)$.

Second, determine the direction of the outward normals of the connection curves at the points determined in the first step. For instance, for the point $\hat{\mathbf{S}}_k(u_{i,0}, 0)$ determined in the first step, since it is also a point of the base surface $\mathbf{S}_0(u, v)$, we identify the point $(u^0_{i,0}, v^0_{i,0})$ in the parameter space of $\mathbf{S}_0(u, v)$ such that $S_0(u^0_{i,0}, v^0_{i,0}) = \hat{\mathbf{S}}_k(u_{i,0}, 0)$. The point $(u^0_{i,0}, v^0_{i,0})$ is located on the parametric connection curve in $S_0(u, v)$'s parameter space. Consequently, one can determine the tangent of the connection curve $\mathbf{T}_0$ at $\mathbf{S}_0(u^0_{i,0}, v^0_{i,0})$ which is the partial derivative of the component surface $\hat{\mathbf{S}}_k(u, v)$ at $\hat{\mathbf{S}}_k(u_{i,0}, 0)$ with respect to u. From the tangent vector of the connection curve $\mathbf{T}_0$ at $\mathbf{S}_0(u^0_{i,0}, v^0_{i,0})$ one can determine the outward normal of the curve at the same point. The direction of the outward normal is the same as the direction of the partial derivative of the component surface $\hat{\mathbf{S}}_k(u, v)$ at $\hat{\mathbf{S}}_k(u_{i,0}, 0)$ with respect to v. The angle between the outward normal at that point and the u axis in the parameter space is noted α^k_i.

The outward normals of the connection curve $\mathbf{T}_1$ at the points determined in the first step can be determined similarly and the angles between the outward normals and the v axis in the parameter space are denoted β^k_i, $k = 0, 1, ..., N-1$, $i = 0, 1, ..., m_k$.

The continuity constraints are then set up as follows:

$$\hat{\mathbf{S}}_k(u^k_{i,0}, 0) = \mathbf{S}_0(u^0_{i,0}, v^0_{i,0}) \tag{16}$$

$$\hat{\mathbf{S}}_k(u^k_{i,m_k}, 1) = \mathbf{S}_1(u^1_{i,m_1}, v^1_{i,m_1}) \tag{17}$$

$$\begin{aligned}\frac{\partial \hat{\mathbf{S}}_k}{\partial v}(u^k_{i,0}, 0) = w_1[&\frac{\partial \mathbf{S}_0}{\partial u}(u^0_{i,0}, v^0_{i,0}) cos\alpha^k_i \\ &+ \frac{\partial \mathbf{S}_0}{\partial v}(u^0_{i,0}, v^0_{i,0}) sin\alpha^k_i]\end{aligned} \tag{18}$$

$$\begin{aligned}\frac{\partial \hat{\mathbf{S}}_k}{\partial v}(u^k_{i,m_k}, 1) = w_2[&\frac{\partial \mathbf{S}_1}{\partial u}(u^1_{i,m_1}, v^1_{i,m_1}) cos\beta^k_i \\ &+ \frac{\partial \mathbf{S}_1}{\partial v}(u^1_{i,m_1}, v^1_{i,m_1}) sin\beta^k_i]\end{aligned} \tag{19}$$

where $k = 0, 1, ..., N-1$, $i = 0, 1, ..., m_k$, and w_1 and w_2 are tension parameters defined in Section 5. Note that the connection curves usually have different lengths. This makes it difficult to generate an appropriate connection surface with C^1 continuity. The purpose of the tension parameters in the above equations is to ensure a G^1 continuity between the connection surface and the the base surfaces and in the meanwhile guarantee a proper shape of the connection surface. The values of the tension parameters should be determined by the designer during the design procedure.

7 Shape Control

In Section 5, two numbers w_1 and w_2, called tension parameters, are introduced into the second and third control points of the profile curve for each component surface. These two parameters

have great influence on the shape of the resulting connection surface. A guideline in selecting the values of these parameters will be given below. Note that when $w_1 = w_2 = 1$, the connection surface has *pseudo-C^1* continuity with the base surfaces S_0 and S_1.

Let H_s be the shortest distance between the two connection curves. For each base surface, find the largest first derivative along the connection curve and denote it by D_l $(l = 0, 1)$,

$$D_l = max\{S_u^l(u(t), v(t)), S_v^l(u(t), v(t))\}$$

where $(u(t), v(t))$ is the parameter of the connection curve and $t \in [0, 1]$. A general guideline for avoiding abnormal connection surface shape is to choose w_0 and w_1 satisfying the following conditions:

$$w_1 D_0 + w_2 D_1 \leq 3H_s$$

$$w_1 > 0$$

$$w_2 > 0$$

If $w_1 = w_2$, then we must have

$$w_1 = w_2 \leq \frac{3H_s}{D_0 + D_1}.$$

8 Shape Optimization

Optimization techniques have been widely used in surface modification and design [3][4] [18][22][?]. An important part of the optimization process is the selection of the objective function. A quadratic objective function will induce a system of linear equations and, consequently, is suitable for computation process. One should try to use a quadratic objective function whenever it is possible. In the following, we will outline the optimization process used in this paper for the smoothing of the connection surface. The optimization process of the base surfaces (Section 4) can be performed similarly.

Let $\hat{\mathbf{S}}(u, v)$ and $\mathbf{S}(u, v)$ denote the initial connection surface and the modified version of the connection surface, respectively. $\mathbf{S}$ is called the *target surface*. The difference between the target surface and the initial surface, called the *displacement function*, is denoted $\mathbf{V}(u, v)$.

$$V(u, v) = (S - \hat{S})(u, v) \tag{20}$$

Based on the theory of thin plate deformation, the energy of a displacement function is defined as follows:

$$E(\mathbf{V}) = \frac{1}{2} \int \int_D F(u, v)\, dudv \tag{21}$$

where D is the parameter space of the surface, and

$$F(u, v) = \alpha F_1(u, v) + \beta F_2(u, v) + \gamma F_3(u, v) \tag{22}$$

with $F_1(u,v)$, $F_2(u,v)$ and $F_3(u,v)$ being the *bending*, *stretching* and *spring* components of the deformation process, respectively. These quantity are defined as follows:

$$\begin{aligned} F_1(u,v) &= (\frac{\partial^2 \mathbf{V}}{\partial u^2})^2 + (\frac{\partial^2 \mathbf{V}}{\partial v^2})^2 + (\frac{\partial^2 \mathbf{V}}{\partial u \partial v})^2 + (\frac{\partial^2 \mathbf{V}}{\partial u^2})(\frac{\partial^2 \mathbf{V}}{\partial v^2}) \\ F_2(u,v) &= (\frac{\partial \mathbf{V}}{\partial u})^2 + (\frac{\partial \mathbf{V}}{\partial v})^2 + (\frac{\partial \mathbf{V}}{\partial u})(\frac{\partial \mathbf{V}}{\partial v}) \\ F_3(u,v) &= \mathbf{V}^2 \end{aligned} \tag{23}$$

They have impact on the amount of surface displacement, variation of surface area, and distribution of surface curvature, respectively. α, β and γ are the weights of these effects on the deformation energy. A study on the determination of these weights can be found in [**?**].

By substituting the representations of the initial connection surface $\hat{S}$ and the target surface S into eqs. (23) and then (21), the energy function can be expressed as a quadratic function as follows:

$$E(\mathbf{Q} - \hat{\mathbf{Q}}) = \frac{1}{2}[\mathbf{Q} - \hat{\mathbf{Q}}]^\top A[\mathbf{Q} - \hat{\mathbf{Q}}] \tag{24}$$

where $\mathbf{Q}$ and $\hat{\mathbf{Q}}$ are the control points of the target surface and the initial connection surface, respectively, and A is a constant matrix defined by the basis functions of the NURBS surface.

The internal and external continuity constraints obtained in the previous section can be expressed as a set of linear equations as follows:

$$B\mathbf{Q} = \mathbf{b} \tag{25}$$

where $\mathbf{Q}$ is the control points of $\hat{\mathbf{S}}$ to be determined, and B and $\mathbf{b}$ are constant matrices.

One then solve this system using the Lagrange Multiplier method. Since the objective function in (24) is quadratic and the constraint equations (24) are linear, the final system to be solved is linear.

To avoid solving an over-determined system, the initial surface sometimes needs to be subdivided. The depth of the subdivision process can be determined by requiring the number of control points of the surface to be larger than the number of constraints.

9 Implementation

The proposed technique has been implemented in Java on a UNIX platform using OpenGL as the supporting graphics system. Test results on four data sets are presented here.

The first result, shown in Figure 4, is to connect two base surfaces along concave connection curves. The connection surface connects the interior portion of the connection curve of one base surface with the exterior portion of the connection curve of another base surface. The tension control parameters are $w_1 = 0.5$ and $w_2 = 0.5$. This is a typical example for feature based shape design in industry.

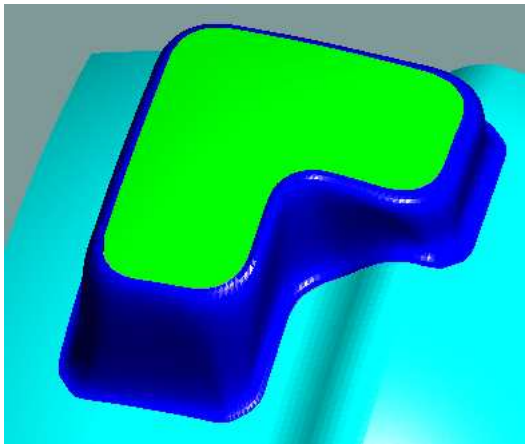

Figure 4: Connecting two general surfaces.

The second case is to show the robustness of the new approach by connecting an elliptic cylinder with a bended base surface (Figure 5). The tension control parameters are $w_1 = 0.33$ and $w_2 = 0.33$. This is an example of classic blending (filleting) process.

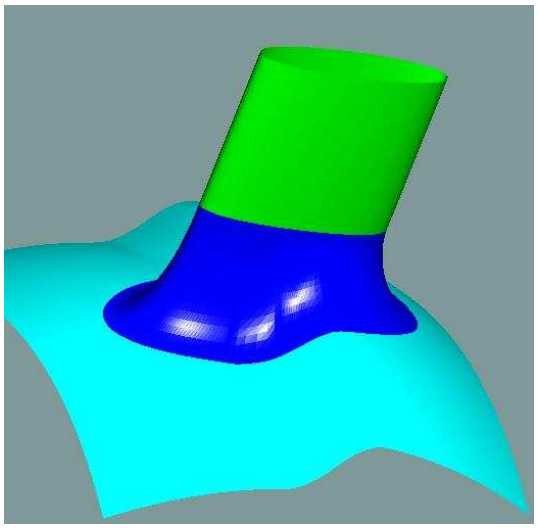

Figure 5: An elliptic cylinder connected with a surface.

The third case (Figures 6 and 7) is to show effect of the tension parameters on the shape of the connection surface. Two elliptic cylinders with different orientations are connected using different tension parameters. In Figure 6, both tension parameters are set to 0.1 while the tension parameters in Figure 7 are both set to 1.0. The results show that larger tension parameters usually generate smoother connection surfaces.

Tha last case is a comparison of the new approach (Figure 8) with Filip's Hermite blending approach (Figure 9). Since the Hermite blending approach is actually piecewise G^1 only, the

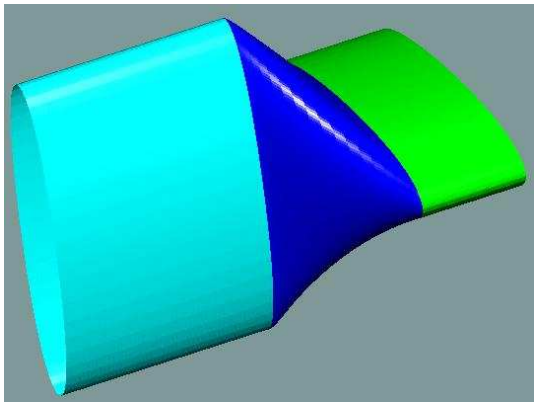

Figure 6: Connecting two cylinders with $w_1 = w_2 = 0.1$.

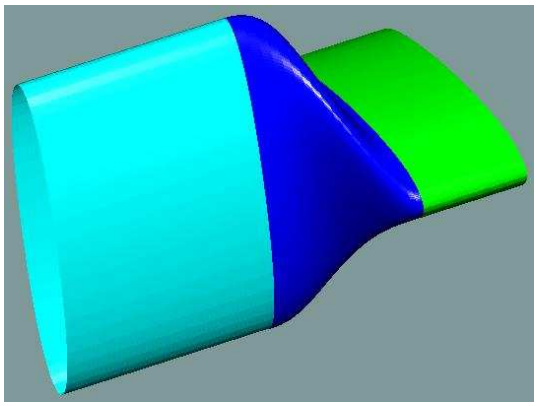

Figure 7: Connecting two cylinders with $w_1 = w_2 = 1.0$.

smoothness of the result shown in Figure 9 is not as good as the one shown in Figure 8, as can be seen from the highlights on the resulting connection surfaces.

All the test cases are carried out on an SGI machine using FFODS (Free-Form Object Design System) developed by the Graphics & Geometric Modeling Lab of the University of Kentucky.

10 Conclusion

Surface connection is a widely used process in automotive and aerospace industries, as well as computer animation and civil engineering. The technique proposed in this paper provides a solution for a general indirect connection environment. The new approach is promising in that it has the following advantages:

1. providing the users with more flexibility in adjusting the shape of the connection surface;

2. the NURBS representation of the connection surface is compatible with most of the current

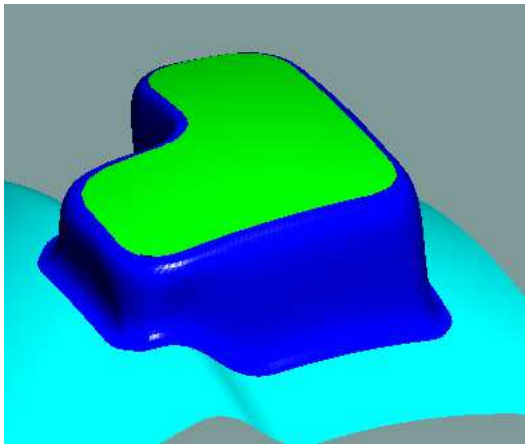

Figure 8: The new approach.

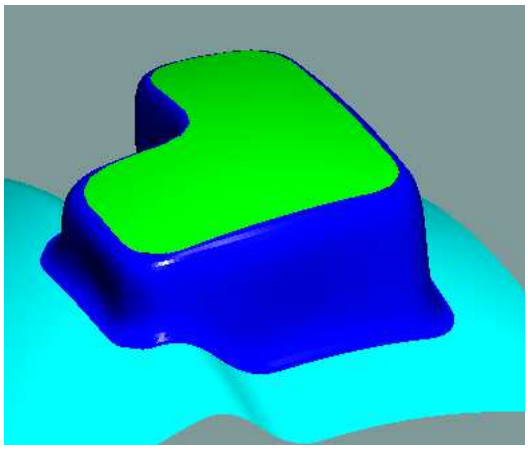

Figure 9: The Hermite blending approach.

data-exchange standards;

3. including the classical blending as a special case and yet allowing more flexibility on the setting of the rail curves;

4. providing a smoother shape of the connection surface through an energy optimization process.

The new approach takes more space for internal representation because the connection surface is a composition of many small Bézier patches. But this seems to be a reasonable price to pay for gaining efficiency and stability in the computation and rendering processes.

As far as future work is concerned, it seems that the presented method can be used for three-way and four-way connection as well. The study of such an extension will be a future research

topic.

References

[1] Bien, A.P. and Cheng, F., A blending model for parametrically defined geometric objects, *Proc. 1st ACM Symposium on Solid Modeling and Applications*, June 5-7, 1991, Austin, Texas, 339-347.

[2] Bloor, M.I.G. and Wilson, M.J., Generating Blend surfaces using partial differential equations, *Computer-Aided Design* 21,3 (1989), 165-171.

[3] Celniker, G. and Gossard, D., Deformable curve and surface finite elements for free form shape design, *Computer Graphics* 25,4 (1991), 257-266.

[4] Celniker, G. and Welch, W., Linear constraints for deformable B-spline surfaces, *Proc. Symposium on Interactive 3D Graphics*, ACM, New York, 1992, 165-170.

[5] Charrot, P. and Gregory, J., A pentagonal surface patch for computer aided geometric design, *Computer Aided Geometric Design* 1 (1984), 87-94.

[6] Chiyokura, H., An Extneded Rounding Operation for Modeling Solids with Free-form Surfaces, *IEEE Computer Graphics & Applications* 7 (1987), 27-36.

[7] Faux, I.D. and Pratt, M.J., *Computational Geometry for Design and Manufacture*, John Wiley, New York, 1979.

[8] Filip, D. J., Blending parameteric surfaces, *ACM Trans. on Graphics*, 8, 3 (1989), 164-173.

[9] Filkins,P. C., Tuohy, S. T., Patrikalakis, N. M., Computational methods for blending surface approximation, *Engineering with Computers*, 9, 1 (1993), 49-62.

[10] Hartmann, E., Blending an implicit with a parametric surface, *Computer Aided Geometric Design* 12, (1995), 825-835.

[11] Hartmann, E., G_n-blending with Rolling Ball Contact Curves, Proceedings Geometric Modeling and Processing 2000 Theory and Application, 10-12 April 2000, Hong Kong, 385-389.

[12] Hoffmann, C.M. and Hopcroft, J., Automatic Surface Generation in Computer Aided Design, *The Visual Computer* 1,2 (1985), 92-100.

[13] Hoffmann, C. and Hopcroft, J., The potential method for blending surfaces and corners, in Farin, G. ed., *Geometric Modeling, Algorithms and New Trends*, SIAM, Philadelphia, PA, 1987, 347-366.

[14] Koparkar, P., Parametric Blending Using Fanout Surfaces, *Proc. 1st ACM Symposium on Solid Modeling and Applications*, June 5-7, 1991, Austin, TX, 317-327.

[15] Lee, E.T.Y., Choosing nodes in parametric curve interpolation, *Computer Aided Design* 21 (1987), 363-370.

[16] Loop, C.T. and DeRose, T.D. (1989), A Multisided Generalization of Bézier Surfaces, *ACM Trans. Graphics* 8,3 (1989), 204-234.

[17] Loop, C.T. and DeRose, T.D. (1990), Generalized B-Spline Surfaces of Arbitrary Topology, *Computer Graphics* 25,4 (1990), 347-356.

[18] Terzopoulos, D. and Qin, H., Dynamic NURBS with Geometric Constraints for interactive Sculpting, *ACM Transactions on Graphics* 13,2 (1994), 103-136.

[19] Vida, J., Martin, R.R., Varady, T., A survey of blending methods that use parametric surfaces *Computer Aided Design* 26 (1994), 341-365.

[20] Warren, J., Blending Algebraic Surfaces, *ACM Trans. Graphics* 8,4 (1989), 263-278.

[21] Welch, W., and Witkin, A., Variational surface modeling, *Computer Graphics* 26,2 (1992), 157-166.

[22] Zhang, P., Zhang, C. and Cheng, F., Constrainted Shape Scaling of Trimmed NURBS Surfaces, Proc. 1999 ASME Design Theory and Methodology Conference, Las Vegas, Nevada, 1999.

[23] Zhang, C.,Zhang, P. and Cheng, F., Constrainted Shape Scaling of Trimmed NURBS Surfaces based on Fix-and-Stretch Approach, *Computer Aided Design* 33,1 (January 2001), 103-112.